Proc. Earthquake Engineering in the 21st Century, Skopje-Ohrid, Macedonia, August 27-September 1, 2005,
(Commemorating the 40th anniversary of IZIIS)
Keynote lecture

POWER DESIGN METHOD

Mihailo D. Trifunac

University of Southern California, Dept. of Civil and Envir. Eng., KAP 216D, Los Angeles, CA, U.S.A., E-mail: trifunac@usc.edu

"The problem of designing structures to withstand destructive earthquakes is not in a very satisfactory condition. On the one hand engineers do not know what characteristics of the ground motion are responsible for destruction, and on the other hand seismologists have no measurements of seismic motion which are sufficiently adequate to serve for design, even if the destructive characteristics were known. Consequently, engineers have been forced to proceed on an empirical basis. From past experience… it has been found that buildings, which are designed to withstand a constant horizontal acceleration of 0.1 gravity are, on the whole, fairly resistant to seismic damage. It is fortunate that such a simple formula works at all, in view of its inadequacy from the point of view of precise computation. We know that seismic motions do not exhibit constant accelerations; that instead they are made up of exceedingly variable oscillatory movements. A formula based upon constant acceleration may thus lead to large errors, especially when applied to new types of structures which have not been tested in actual earthquakes." Benioff [1934]

ABSTRACT

This paper begins by noting the limitations of the classical Response Spectrum Method (RSM) for design of earthquake resistant structures in the near field of strong earthquakes. RSM is based on the largest peak of the relative response, and does not consider the duration of strong motion. Then the elementary principles of Power Design Method (PDM) are introduced, based on the power of incident waves of strong ground motion in the near field. It is shown how the rate of incident wave energy (power) can be compared with the maximum rate at which the structure can absorb the incident wave energy via non-linear response, and how equating these two can be used to select the design parameters. The advantages of using the power of incident strong motion for design of structures are discussed. Recorded response of a seven-story reinforced concrete hotel (VN7SH) in Van Nuys, California, during thirteen earthquakes between 1971, and 1994, damaged during January 1994, Northridge earthquake, is described to illustrate computation of power capacities and demands.

Keywords: Response Spectra, Power of incident waves, Design by maximum drift.

1. INTRODUCTION

The modern era in Earthquake Engineering begins with the formulation of the concept of Response Spectrum by Biot [1932, 1933, 1934]. He presented the general theory, analyzed the first recorded accelerograms [Biot, 1941] and formulated the principles of response spectrum superposition [Biot, 1942]. Today, three quarters of a century later, his ideas still govern the principles of earthquake resistant design [Trifunac, 2003; 2005].

The method of response spectrum superposition woks well for design of structures expected to vibrate without damage during the largest possible levels of shaking. However, pragmatic considerations, analyses of uncertainties, and minimization of cost result in the design of structures, that may experience damage from rare and very strong earthquake shaking. Thus, during the last 40 years, many modifications and "corrections" have been introduced into the response spectrum method to reconcile its *linear* nature with its desired *nonlinear* use in design.

Well-designed structures are expected to have *ductile behavior* during the largest credible shaking, and *large energy reserve* to at least delay failure if it cannot be avoided. As the structure finally enters large nonlinear levels of response, it absorbs the excess of the input energy through ductile deformation of its components. Thus, it is logical to formulate earthquake resistant design procedures in terms of the energy driving this process. From the mechanics point of view, this brings nothing new, since the energy equations can be derived directly from the Newton's second law. The advantage of using energy is that the duration of strong motion, the number of cycles to failure and dynamic instability, all can be addressed directly and explicitly. This, of course, requires scaling of the earthquake source and of the attenuation of strong motion to be described in terms of its wave energy.

In 1934, Benioff proposed the seismic destructiveness to be measured in terms of the response energy, by computing the area under the relative displacement response spectrum. It can be shown that his result can be related to the energy of strong motion [Arias, 1970; Trifunac and Brady, 1975a]. Thus an alternative to the spectral method in earthquake resistant design is to analyze the flow of energy during strong motion. The principal stages of earthquake energy flow are at the earthquake source, along the propagation path, and finally the remaining energy leading to relative response of the structure. The losses of energy along its propagation path must be considered. These losses must be accounted for to properly quantify the remaining energy, which will excite the relative response of the structure [Trifunac et al., 2001e].

The seismological and earthquake engineering characterizations of the earthquake source begin by estimating its "size". For centuries this was performed by means of earthquake intensity scales, which are not instrumental and are based on human description of the effects of earthquakes [Richter, 1958; Trifunac and Brady, 1975b]. In the early 1930's, the first instrumental scale – the local earthquake magnitude M_L was introduced in southern California [Richter, 1936; 1958]. Few years later, it was followed by the surface wave magnitude M_s [Gutenberg and Richter, 1956a,b], and more recently by the moment magnitude $M_w = (\log_{10} M_0 - 16)/1.5$ (where M_0 is seismic moment), and by the strong motion magnitude M_L^{SM} [Trifunac, 1991]. The seismic energy associated with elastic waves radiated from the source, E_s, (Gutenberg and Richter, 1956a,b) has also been used to compare "sizes" of

different earthquakes. The seismic energy, E_s, radiated from the earthquake source is attenuated with increasing epicentral distance, r, through the mechanisms of inelastic attenuation [Trifunac, 1994], scattering, and geometric spreading. In the near-field, for distances comparable to the source dimensions, different near-field terms attenuate like r^{-4} and r^{-2} [Haskell, 1969]. The body waves (P- and S-waves) attenuate like r^{-1}, while the surface waves attenuate like $r^{-1/2}$.

The seismic wave energy arriving towards the site is next attenuated by nonlinear response of shallow sediments and soil in the "free-field" [Joyner, 1975; Joyner and Chen, 1975; Trifunac and Todorovska, 1996; 1998; 1999], before it begins to excite the foundation. Once the foundation is excited by the incident waves, the response of the soil-structure-system is initiated. The incident wave energy is further reduced by nonlinear response of soil during soil-structure interaction [Gicev, 2005; Trifunac et al., 1999a,b; 2001a,b], and by radiation damping [Luco et al., 1985; Todorovska and Trifunac, 1991; Hayir et al., 2001].

Engineering analyses of seismic energy flow and distribution among different aspects of the structural response have been carried out since the mid 1950's. A review of this subject and examples describing the *limit-state* design of buildings can be found in the book by Akiyama [1985], and in collected papers edited by Fajfar and Krawinkler [1992], for example. In most engineering studies, the analysis begins by integrating the differential equation of dynamic equilibrium of an equivalent single degree of freedom system with respect to displacement, which results in

$$E_I = E_K + E_\xi + E_E + E_H \qquad (1)$$

where E_I is the input energy, E_K is the kinetic energy, E_ξ is the damping energy, E_E is the elastic strain energy, and E_H is the hysteretic energy [e.g Uang and Bertero, 1988].

Common problems with this approach are that the computed energy is essentially converted to peak relative velocity [Akiyama, 1985], thus using energy merely to compute equivalent relative velocity spectra. Further the effects of soil-structure interaction are ignored, and because of that significant mechanisms of energy loss (nonlinear response of the soil and radiation damping) are thus neglected, leading to erroneous inferences about the structural response. Other simplifications and important omissions in equation (1) are that the dynamic instability and the effects of gravity on nonlinear response are usually ignored [Husid, 1967; Lee, 1979; Todorovska and Trifunac 1991, 1993].

Trifunac et al., (2001e) reviewed the seismological aspects of empirical scaling of seismic wave energy, E_s, and showed how the radiated energy can be represented by functionals of strong ground motion [Trifunac, 1989; 1993]. They described the energy propagation and attenuation with distance, and illustrated it for the three-dimensional geological structure of Los Angeles basin during the 1994 Northridge, California earthquake. Then they described the seismic energy flow through the response of soil-foundation-structure systems, analyzed the energy available to excite the structure, and finally the relative response of the structure.

Figure 1 illustrates the cumulative wave energies recorded at a building site during two hypothetical earthquakes, E1 an E2, and presents the conceptual framework, which can be used for development of the power design method. E1 results in a larger total shaking energy at the site, and has long duration of shaking leading to relatively small average power, P1. E2 leads to smaller total shaking energy at

the site, but has short duration and thus larger power, P2. The power capacity of a structure cannot be described by one unique cumulative curve, as this depends on the time history of shaking. For the purposes of this example, the line labeled "capacity envelope of the structure" can be thought of as an envelope of all possible cumulative energy paths for the response of this structure. Figure 1 implies that E1 will not damage this structure, but E2 will. Hence, *for a given structure, it is not the total energy of an earthquake event (and the equivalent energy compatible relative velocity spectrum), but the rate with which this energy arrives and shakes the structure, that is essential for the design of the required power capacity of the structure to withstand this shaking, and to control the level of damage.*

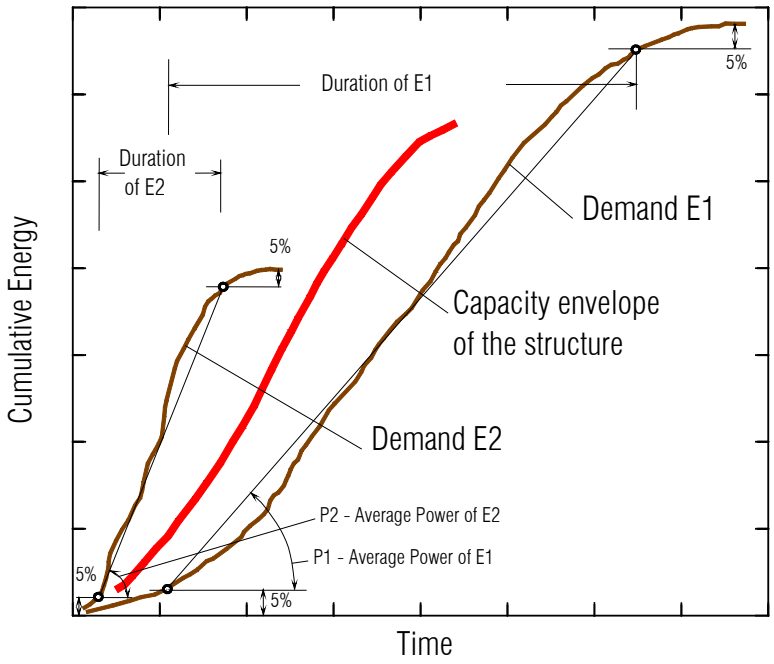

Fig.1 Comparison of strong motion demands E1 and E2 with an envelope of structural capacity.

In this paper elementary aspects of design, based on the power of the incident wave pulses, are illustrated. It will be shown how this power can be compared with the capacity of the structure to absorb the incident wave energy, and the advantages of using the computed power of incident strong motion for design will be described.

2. LIMITATIONS OF THE EIGENFUNCION EXPANSION

At present much of the earthquake resistant design continues to be based on the linear concepts of relative response spectrum, and on mode superposition. However, as used in practice, the modal approach has a low-pass filtering effect on the end result (the computed peak relative displacement at each floor) because in design the higher modes are usually neglected. Therefore, in typical earthquake engineering applications the modal approach is not able to represent the early transient response, particularly for excitation by high frequency pulses in the near-field, with large peak velocities, which are associated with high stress drop at the near asperities, and with duration short relative to the travel time required for an incident wave to reach the top of the building ($t < H / \beta_b$; H and β_b are the height and vertical shear wave velocity in the building). As the modes of vibration are standing waves, and result from constructive interference of the incoming wave and the wave reflected from the top of the building, the building starts vibrating in the first mode only after time $t = 2H/\beta_b$ has elapsed. Although, in principle, the representation of the response as a linear combination of the modal responses is mathematically complete, short "impulsive" representation would require considering

many modes (infinitely many for a continuous model), which is impractical. The wave propagation methods are therefore more *natural* for representing the *early* transient response, and should be used to find solutions where the modal approach is limited.

3. POWER AND ELEMENTARY ASPECTS OF TRANSIENT DESIGN

Wave propagation models of buildings have been used for many years [Kanai, 1965], but are only recently beginning to be verified against observations [Ivanovic et al. 1999;2000; Todorovska et al., 2001a,b,c; Trifunac and Todorovska, 2001; Trifunac et al., 2001d]. Continuous, 2-D wave propagation models (homogeneous, horizontally layered and vertically layered shear plates) can be employed to study the effects of traveling waves on the response of long buildings [Todorovska et al., 1988; Todorovska and Trifunac, 1989; 1990a,b; Todorovska and Lee, 1989]. Discrete-time 1-D wave propagation models were proposed to study the response of tall buildings [Safak, 1998], and 2-D finite difference methods were used to study linear and non-linear soil-structure interaction (Gicev, 2005).

In the following the elementary principles of wave propagation through a homogeneous shear beam model will be used to derive approximate relationships between the power of an incident pulse of strong ground motion (with peak velocity $v_{G,\max}$ in the free-field), and of the building response.

3.1 Velocity Pulses

Strong ground motion can be viewed as resulting from a sequence of pulses emitted from failing asperities on the fault surface [Trifunac, 1972a,b; 1974;1998]. Through multiple arrivals with different source to station paths and scattering, the strong motion observed at a site assumes the appearance of irregular oscillations in time, but usually preserves one or several larger and long velocity "pulses". These pulses are "spread out" in time due to multiple arrival paths and dispersion, but do appear systematically in recordings at adjacent stations, up to the epicentral distances approaching 100 km [Todorovska and Trifunac, 1997a,b; Trifunac et al., 1998].

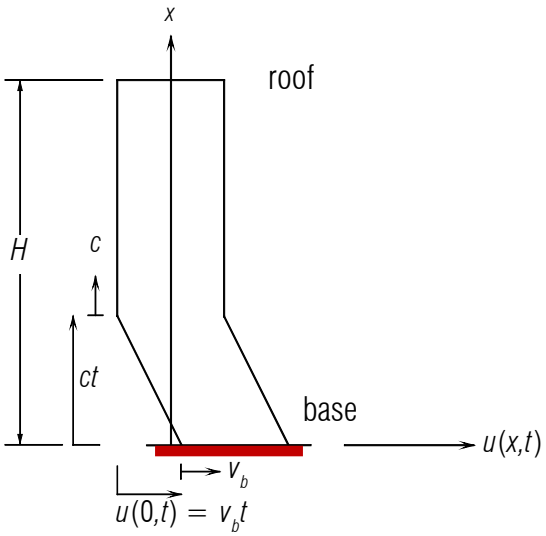

Fig. 2 Wave caused by a sudden movement at the base of a shear building, for constant velocity pulse with amplitude v_b and for time $t < t_0$ (= pulse duration).

As a first approximation, consider the motion at the base of the building to be a velocity pulse with amplitude v_b and duration t_0. For small t_0, this pulse approximates a delta function, and can be used as a building block to represent more general velocity pulses in input motion. For an elastic building on rigid soil (i.e. no soil structure interaction), a velocity pulse with amplitude $v_b = v_{G,\max}$, will create a wave propagating up the building with velocity c (see Fig. 2). For times shorter than H/c and for elastic strain γ ($\gamma = \partial u/\partial x = v_b/c$), i.e. displacement $u(x,t)$ smaller than the elastic limit u_y (Fig. 3),

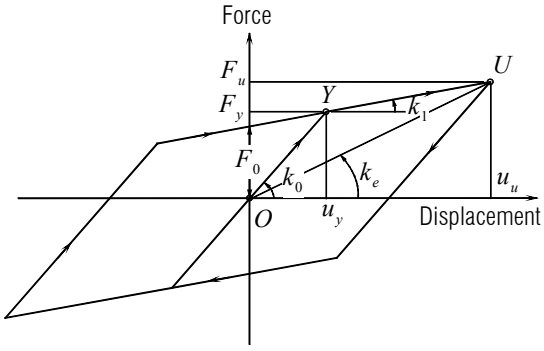

Fig. 3 Bilinear force-displacement representation of a shear beam building experiencing non-linear response

the wave propagating up into the building will be defined by a straight line

$$u(x,t) = \begin{cases} v_b t - \dfrac{v_b}{c} x & \text{, for } 0 \le x \le ct \\ 0 & \text{, for } x > ct \end{cases} \qquad (2)$$

During reflection from the stress-free top of the building, the incident wave from below and the reflected wave from above will interfere leading to double amplitude at the roof. The propagation of the energy of the pulse will continue downward, as a linear wave, as long as the incident wave amplitude is smaller than $u_y/2$.

Figure 4 illustrates the peak drift amplitudes (v_b/c) in a shear beam model of a building, assuming c = 100 m/s, short transient pulses, and linear response. For twelve earthquakes (Table 1 and Figure 5), the maximum drift at the base of structure is plotted versus v_b (solid points). For the Landers, San Fernando and Northridge earthquakes, the maximum drift, at the roof, is also shown ($2v_b/c$). It is seen that the maximum drift at base occurs during the Northridge earthquake and is approximately 0.5%, while at roof it is equal to about 1%.

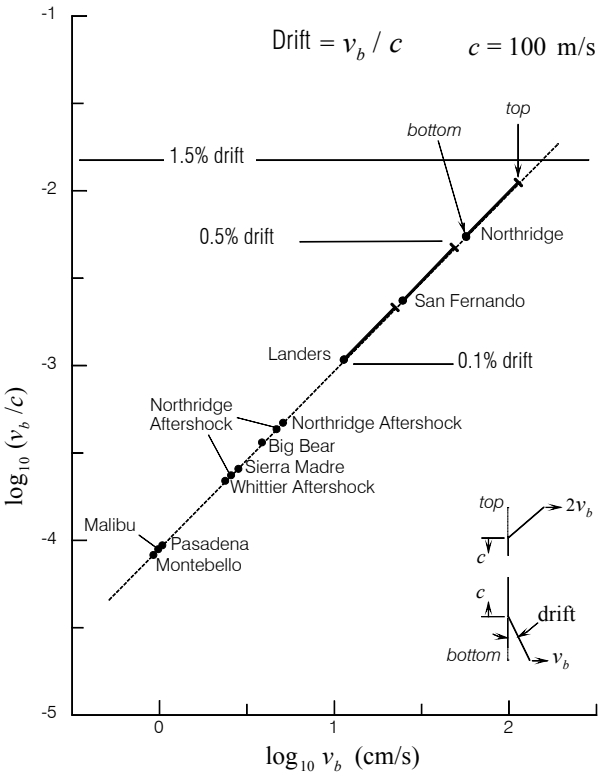

Fig. 4 Drift amplitudes in a shear beam model, with linear shear wave velocity c = 100 m/s.

For a building supported by flexible soil, the soil-structure interaction will lead to horizontal and rocking deformations of the soil, and in general this will modify and usually reduce the amplitude v_b of the strong motion pulse entering the structure [Gicev, 2005]. Partitioning of the incident wave energy into horizontal and rocking motions of the building-foundation-soil system and scattering of the incident wave from the foundation will thus change the energy available to cause relative deformation of the structure.

The presence of the foundation within the soil creates an impedance jump for incident wave motion, and this causes scattering of the incident waves [Trifunac 1972c; Iguchi and Luco, 1982; Lee et al., 1982; Moslem and Trifunac, 1987; Todorovska and Trifunac, 1990a,b,c ; 1991; 1992; 1993; Trifunac et al.,

2001c]. Figure 6, redrawn from Gicev [2005] illustrates the reduction of incident amplitude of $v_{G,\max}$ through scattering and refraction for a two-dimensional soil-foundation-building model. It is seen that for the dimensionless frequencies higher than about 1.0, $v_b / v_{G,\max}$ is reduced to between 0.2 and 0.4.

3.2 Power Demand and Capacity of Structure to dissipate Energy

We assume that the velocity pulse leaving foundation and entering the structure (as shown in Fig. 2) has amplitude v_b. When the soil-structure interaction can be neglected, $v_b = v_{G,\max}$, and when it redistributes the incident wave energy, $v_b = P\, v_{G,\max}$, where $P < 1$ (Figure 6; Trifunac et al., 2001e; Gicev, 2005). Assuming that the soil-foundation system has equivalent density ρ_e and shear wave velocity β_e, the energy carried by the incident waves, per unit time and across unit area normal to the direction of propagation, is $\rho_e \beta_e v_b^2$.

Table 1 Peak ground velocity ($v_{G,\max}$) during thirteen earthquakes.

Earthquake	Date	M_L	**R** (km)	NS	EW
				$v_{G,\max}$ (cm/s)	$v_{G,\max}$ (cm/s)
San Fernando	02/09/1971	6.6	10*	29.28	23.72
Whittier Narrows	10/01/1987	5.9	41	8.14	--
Whittier 12th Aft.	10/04/1987	5.3	41	1.33	2.18
Pasadena	12/03/1988	4.9	32	1.46	0.94
Malibu	01/19/1989	5.0	35	0.93	0.96
Montebello	06/12/1989	4.6	34	0.45	0.85
Sierra Madre	06/28/1991	5.8	44	4.40	2.78
Landers	06/28/1992	7.5	186	10.42	10.64
Big Bear	06/28/1992	6.5	149	3.87	3.58
Northridge	01/17/1994	6.4	4	35.32	50.93
Northridge Mar. Aft.	03/10/1994	5.2	1	7.61	4.83
Northridge Mar. Aft.	03/10/1994	5.2	1	2.58	4.21
Northridge Dec. Aft.	12/06/1994	4.3	11	2.67	2.41

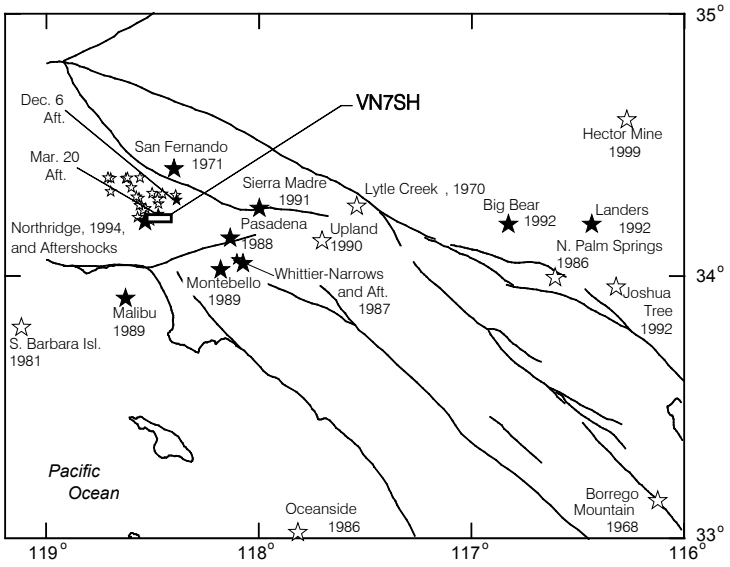

Fig. 5 Southern California earthquakes for which recorded data in VN7SH building has been digitized (solid stars).

With reference to Fig.3, the hysteretic work per one complete cycle of nonlinear relative response of the structure is

$$W_{\square} = 4\, F_0\, (u_u - u_y)\,. \qquad (3)$$

Since

$$F_0 = F_y - k_1\, u_y = (1-\alpha)\, k_0\, u_y\,, \qquad (4)$$

defining,

$$k_0\, u_y \equiv F_y = m\, a_y\,, \qquad (5)$$

where a_y is static acceleration which produces deflection u_y, $k_1 = \alpha\, k_0$, and using the standard definition of ductility

$$\mu = u_u / u_y\,, \qquad (6)$$

one can write

$$W_{\square} = 4\,(1-\alpha) m_b\, a_y\, (\mu - 1)\, / u_y\,. \qquad (7)$$

We approximate the equivalent stiffness of the nonlinear system by the secant modulus (see Fig. 3)

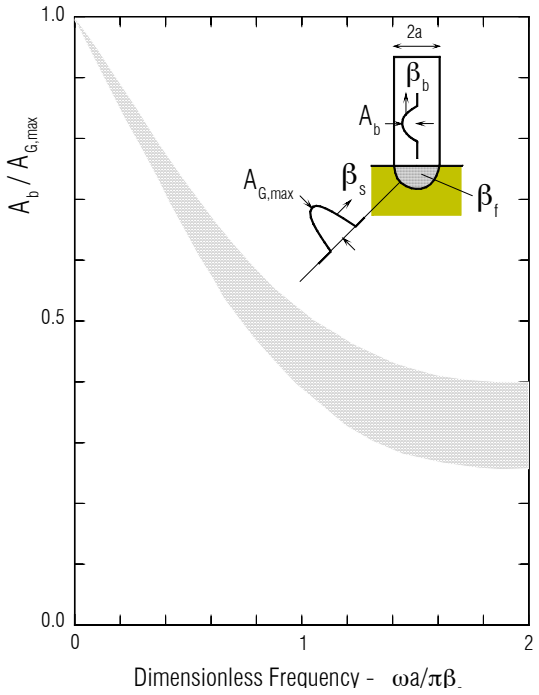

Fig. 6 Reduction of v_b relative to $v_{G,\max}$ caused by scattering and diffraction of incident waves from the foundation, and by refraction from foundation into the building (redrawn from Gicev, 2005).

$$k_e = k_0\left[\frac{1+\alpha(\mu-1)}{\mu}\right] \tag{8}$$

This gives the approximate period of nonlinear oscillator

$$T_e = T_n\,\xi \tag{9}$$

Where

$$\xi = \left[\frac{\mu}{1+\alpha(\mu-1)}\right]^{1/2} . \tag{10}$$

The maximum power the oscillator can absorb during one cycle of response is then

$$W_{\square}/T_e = 4(1-\alpha)(\mu-1)\, m_b\, a_u\, u_y/T_n\xi \tag{11}$$

and since for the first mode of vibration $T_n = 4H/\beta_b$

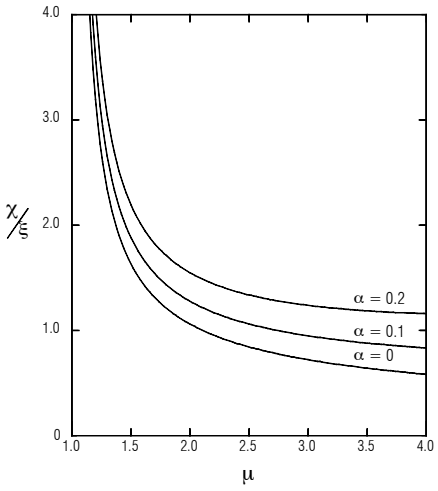

Fig. 7 Plot of χ/ξ versus ductility μ.

$$W_{\square}/T_e = 4(1-\alpha)(\mu-1)\frac{m_b a_y u_y \beta_b}{4H\xi}. \tag{12}$$

To avoid damage, we may require

$$A_b\rho_e\beta_e v_b^2 < (1-\alpha)(\mu-1)\frac{m_b a_y u_y \beta_b}{H\xi} \tag{13}$$

With $m_b = \rho_b HA_b$, Eqn. (13) gives

$$v_b^2 < (1-\alpha)(\mu-1)\frac{\rho_b}{\rho_e}\frac{\beta_b}{\beta_e}\frac{a_y u_y}{\xi} \tag{14}$$

As an illustration, let $u_y = \psi H$, where ψ is the drift angle and H the height of the single story structure. Assuming $\psi = 0.05$ and $H = 3.5$ m, will give $u_y = 0.05 \times 3.5 = 0.175$ m. Also, assume that $a_y = 0.25 \times 9.81$ m/s^2 = 2.45 m/s^2, $\mu = 2$, $\alpha = 0.05$, $\rho_b/\rho_e \sim 0.1$, $\beta_b/\beta_e \sim 0.3$, and finally that $\xi \sim 1$. Then

$v_b^2 < (0.95)(1)(0.1)(0.3)(0.175)2.45 = 122\,\text{cm}^2/\text{s}^2$ or v_b < 11 cm/s. It is interesting to note that for various transient excitations, including earthquakes, serious damage of buildings begins to occur for peak ground velocities exceeding 10-20 cm/s (e.g. see Trifunac and Todorovska, 1997).

Equation (14) can be viewed only as a form of a dimensional analysis of the problem, since v_b will oscillate in time, and since we did not solve the response problem explicitly. Furthermore it is not probable that the incident motion will be so "regular" to allow monotonic completion of the complete hysteretic cycle. Instead, it is more likely that the pulse v_b will be one-directional, with low frequency content, and of considerable duration causing monotonic increase of the relative displacement u. Therefore it is also of interest to examine the relationship of the input power demand relative to the capacity of the structure to absorb this power along the path OYU (as shown in Fig. 3). The work accompanying nonlinear response in going from O to U is

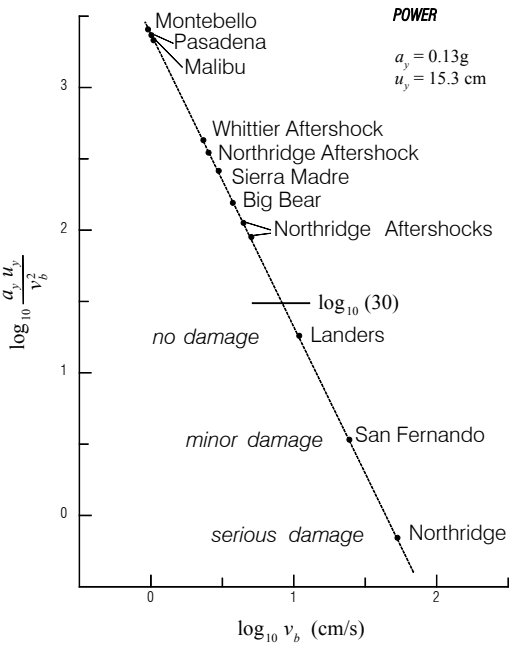

Fig. 8 Plot of $\log_{10}\left(a_y u_y / v_b^2\right)$ versus v_b, assuming a_y = 0.13g, u_y = 15.3 cm (see Fig. 10) and $v_b \sim v_{G,\max}$, for the twelve events in Table 1.

$$W_{\rightarrow} = \frac{1}{2}k_0 u_y^2 + \left(u_u - u_y\right)k_0 u_y + \frac{1}{2}k_1\left(u_u - u_y\right)^2 \quad (15)$$

or

$$W_{\rightarrow} = k_0\left[\frac{1}{2} + (\mu - 1) + \frac{1}{2}\alpha(\mu - 1)^2\right]u_y^2$$

$$= \left[\frac{1}{2} + (\mu - 1) + \frac{1}{2}\alpha(\mu - 1)^2\right]m_b a_y u_y \quad (16)$$

The time required to reach U starting at O is approximately $T_e/4$, and this gives the associated power absorbing capacity of the structure

$$4W_{\rightarrow}/T_n\xi = \left[\frac{1}{2} + (\mu - 1) + \frac{1}{2}\alpha(\mu - 1)^2\right]\frac{m_b a_y u_y 4\beta_b}{4H\xi} \quad (17)$$

Again, recalling that $m_b = A_b H\rho_b$, this requires

$$v_b^2 < \left[\frac{1}{2} + (\mu - 1) + \frac{1}{2}\alpha(\mu - 1)^2\right]\frac{\rho_b}{\rho_e}\frac{\beta_b}{\beta_e}\frac{a_y u_y}{\xi} \quad (18)$$

Comparison with Eqn. (14) shows that

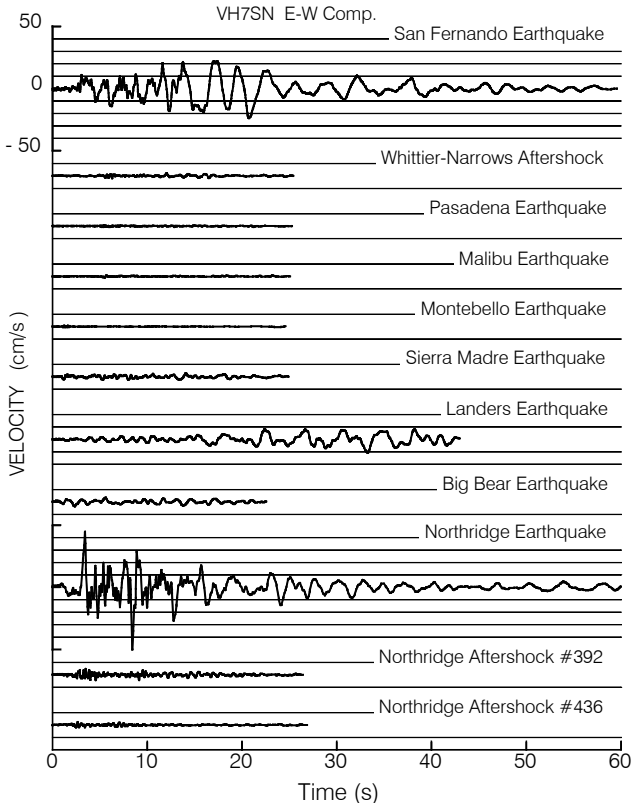

Fig. 9 Corrected velocity at ground level of VN7SH in the EW direction, recorded during eleven earthquakes (see Table 1). During the Whittier-Narrows, 1987, earthquake the EW transducer at the ground floor did not record.

$$\chi = \frac{\frac{1}{2} + (\mu - 1) + \frac{1}{2}\alpha(\mu - 1)^2}{(1-\alpha)(\mu - 1)} > 1 \qquad (19)$$

for $\mu \geq 1$ and $\alpha \geq 0$.

In Fig. 7 we show χ/ξ versus μ and for $0 < \alpha < 0.2$. It is seen that χ/ξ monotonically decreases for increasing μ. For $\mu < 4$, it is greater than 0.5 and for $\alpha \geq 0.2$ it is greater than 1.0. Thus combining Eqns. (14) and (18) and simplifying, we arrive at a remarkably simple criterion for design

$$a_y u_y > c \frac{\rho_e}{\rho_b} \frac{\beta_e}{\beta_b} v_b^2 \qquad (20)$$

where $c \sim 1$ for $\alpha \geq 0.2$. It is seen that as long as $a_y u_y$ satisfies Eqn. (20), the capacity of the structure to absorb the incident power will be adequate and no major damage is to be expected. For large velocity pulses, the damage will occur progressively and will continue to increase with each new additional pulse, which does not satisfy Eqn. (20). With progressing damage, the system parameters will also change (a_y, u_y, β_b) and Eqn. (20) will continue to apply, subject to appropriate modifications.

3.3 A Case Study - Van Nuys Hotel (VN7SH)

Figure 8 shows $\log_{10}(a_y u_y / v_b^2)$ plotted versus $v_{G,\max}$ (assuming that $v_b \approx v_{G,\max}$) for the EW response of VN7SH for 12 events in Table 1 (Fig. 9). Assuming $a_y = 0.13$g, $u_y = 15.3$ cm (see Fig. 10), $c \sim 1$, $\alpha \sim 0.2$, $\rho_e/\rho_b \sim 10$ and $\beta_e/\beta_b \sim 3$ would result in the condition $a_y u_y / v_b^2 > 30$ for no damage to occur. The observations in VN7SH suggest $a_y u_y / v_b^2 \geq 5$ as a criterion for no damage to occur. This is equivalent to the requirement that $v_b \leq 20$ cm/s.

Figure 9 shows the EW velocities recorded in the basement of VN7SH during 11 earthquakes selected from Table 1. It is seen that during the 1971 San Fernando earthquake, the EW ground velocity exceeded 20 cm/s during very short time intervals and only slightly. During the 1994 Northridge earthquake, the EW peak ground velocities were larger, and two large peaks, at 3.45 s and 8.45 s, had

peak amplitudes approaching 50 cm/s.

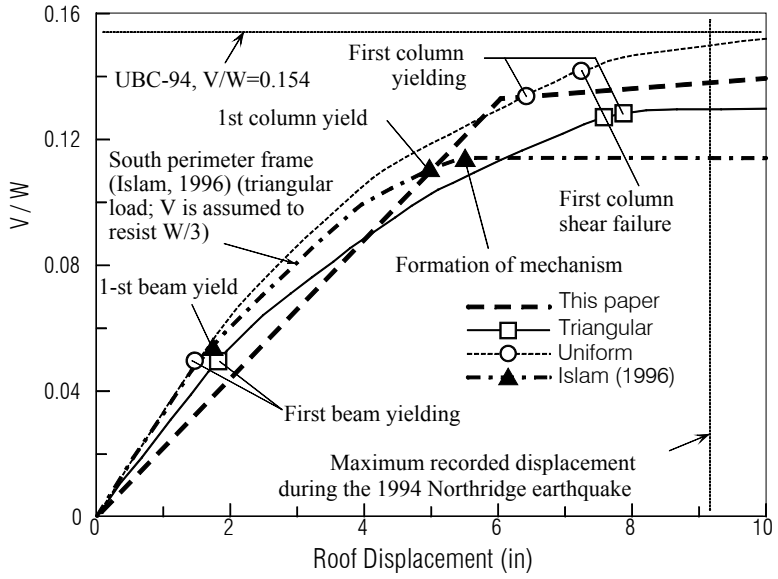

Fig. 10 Base shear (V) coefficient normalized by 1/3 of the total building weight, W, versus EW roof displacement of VN7SH (after Islam [1996] and Li and Jirsa [1998]).

The above values of a_y = 0.13g and u_y = 15.3 cm have been estimated based on nonlinear static push-over analysis of the EW response of VN7SH by Islam [1996] and Li and Jirsa [1998]. Their results are summarized in Fig. 10, showing the base shear coefficient, V/W, where V is the computed base shear, and W is total weight of the building ($W \sim 10^4$ kips), plotted versus roof displacement for triangular and uniform load distribution patterns. Also shown in this figure are the "maximum roof displacement" determined by Islam [1996] and by Li and Jirsa [1998] computed from the recorded data, and the computed UBC-94 base shear $V = 0.154\ W$.

For fixed-base EW response, the two independent estimates of F_y are F_y = 1300 kips (5780 kN) [Li and Jirsa, 1998] and F_y =1140 kips (5070 kN) [Islam, 1996]. Assuming u_y = 15.3 cm, these two estimates imply $F_y u_y$ = 775 to 884 kNm. During 1/4 cycle of the response, assuming linear deformation in the building would result in maximum accumulated potential energy equal to 387 to 442 kNm (see Fig.11, left). For $T_n \sim 0.8$ s, we can estimate the largest power of the EW component of the incident waves which the VN7SH building can take without damage to be 1932 to 2208 kNm/s.

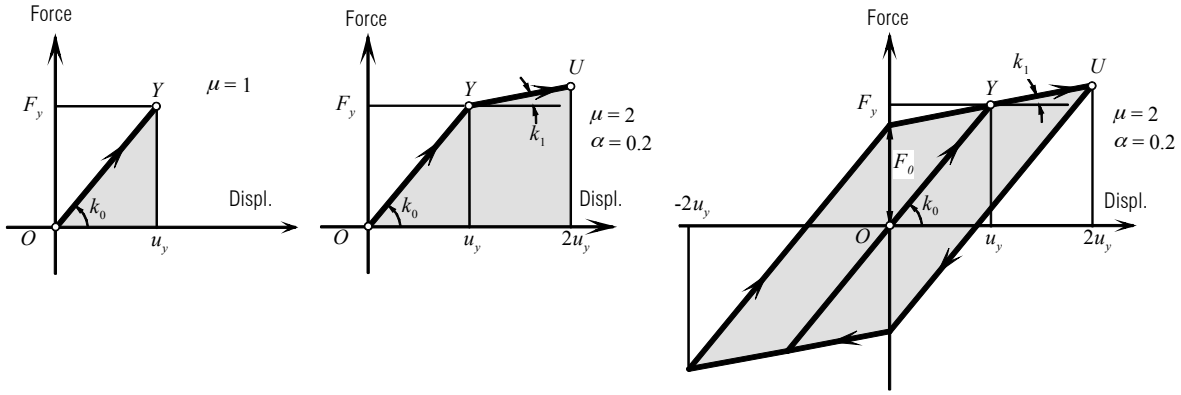

Fig. 11 The shaded areas represent: (left) maximum potential energy associated with linear response; (center) hysteretic energy associated with monotonic nonlinear response; and (right) hysteretic energy associated with oscillatory (periodic, one cycle) excitation.

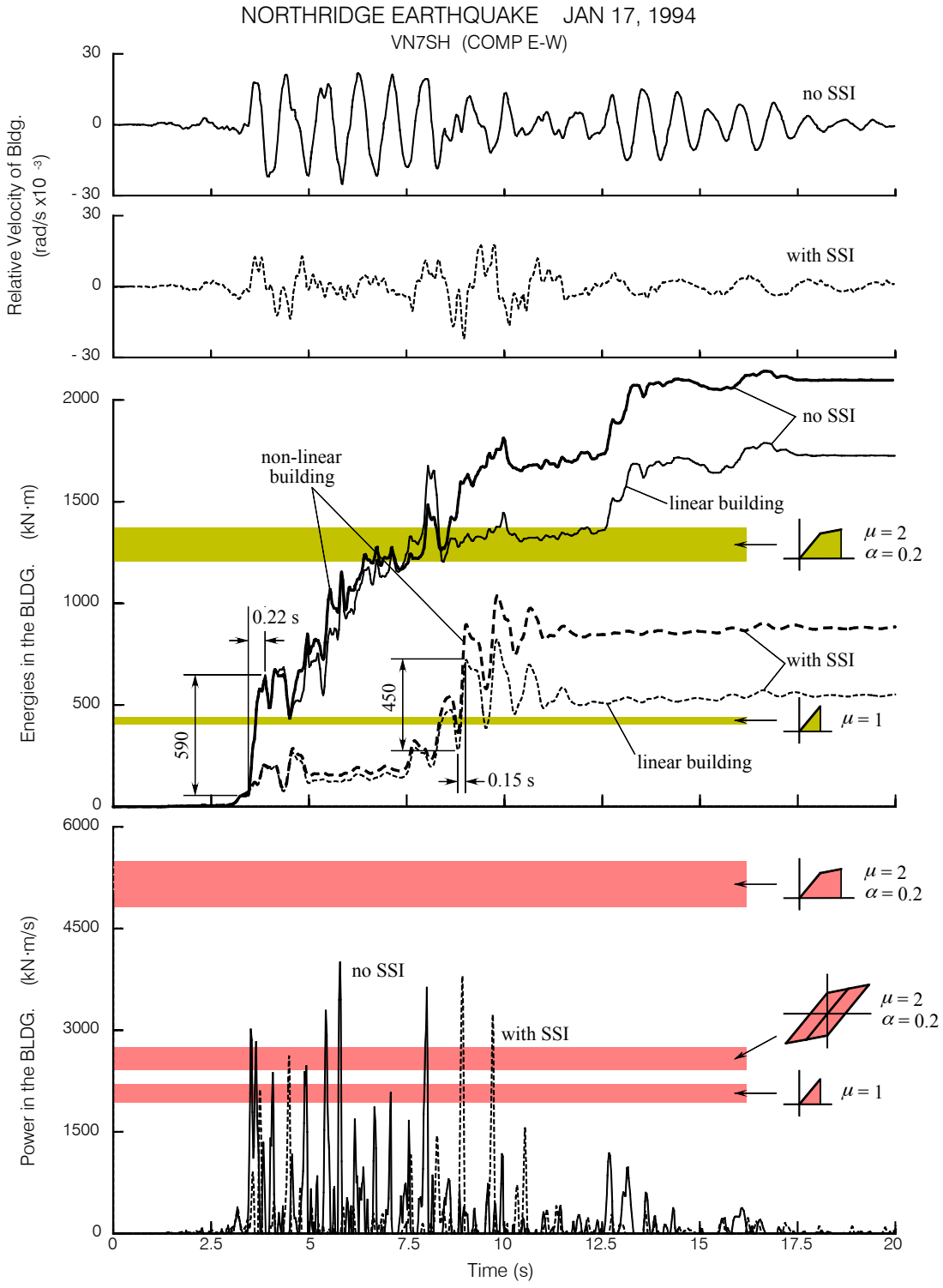

Fig. 12 Comparison of the EW response of VN7SH during the 1994 Northridge earthquake in the presence and absence of soil-structure interaction: (top) relative velocities of the building response; (center) energies of the relative response; and (bottom) power of the relative response.

The time dependent evolution of the energy dissipated by nonlinear building response will depend on the history of the excitation, but several characteristic values can nevertheless be estimated a priori. This is illustrated in Fig. 11. The shaded area in the left figure illustrates the largest potential energy in the oscillator, which is still responding in the linear range of response ($u < u_y$) when $\mu = 1$ and when $F = F_y$. For VN7SH, using static push over analyses of Islam [1996] and Li and Jirsa [1998], for EW response, as indicators of the possible range of F_y, we obtain the estimates of 5070 kN and 5783 kN respectively. A larger and longer lasting incident velocity pulse might force the equivalent oscillator to deform monotonically to say $u = 2\ u_y$ ($\mu = 2$), during $T_e/4$. This case is illustrated in the central part of Fig. 11. Assuming that $\alpha = 0.2$ implies the work dissipated by the hysteresis in going from O to Y to U to be 1240 to 1414 kNm (see Eqn. (16)), and the associated power $4W_{\rightarrow}/T_n\xi$ to be in the range from 4816 to 5492 kNm/s. The right part of Fig. 11 shows the closed hysteretic loop, starting at OYU and returning to Y after one complete cycle lasting $T_n\xi$ s. The work dissipated by such a loop, assuming F_y as above, ($\mu = 2$ and $\alpha = 0.2$) is 2480 to 2829 kNm. The corresponding maximum power this oscillator can dissipate along this path is then 2407 to 2746 kNm/s. These estimates of the building capacity to absorb energy and power are shown by the gray areas in Fig. 11.

Figure 12 (top) shows the relative response of the model with parameters chosen to represent VN7SH. In this figure we compare the relative response assuming fixed-base ("no SSI"), and flexible base ("with SSI"). In the center of Fig. 12 we show the sum of all energies in the relative building response (kinetic, potential and hysteretic, when the building model is linear and nonlinear), for the fixed base model ("no SSI") and in the presence of soil-structure interaction ("with SSI"). It is seen that for the "no SSI" case, a large ground motion pulse starting at about 3.4 s (see Fig. 9) would have resulted in energy jump of about 520 KNm, during about 0.22 s, resulting in input power approaching 3000 kN m/s (see bottom of Fig. 12). This pulse would have deformed the building beyond its linear response range, between 3.5 and 4 seconds into the earthquake (see also Islam, 1996). In the presence of soil structure interaction, the amplitude of the incident wave is reduced, and the building continues to respond in essentially a linear manner until 8.4 s into the earthquake. At about 8.9 s, the SSI model experiences sudden jump in the energy of the relative response (e.g. at 8.9 and 9.7 s) during short "stiff" episodes of response, for example during closure of the gaps between the foundation and the soil. Nevertheless, the benefits of not ignoring SSI are apparent from Fig. 12 (center), which shows that the response energy in the building in this case is reduced by a factor of about 3 due to SSI. The challenge for future research is to quantify such reductions and to show how those can be estimated for use in the design process.

4. SUMMARY AND CONCLUSIONS

Biot's response spectrum method uses characteristic functions (mode shapes) to represent vibration of multi-degree-of-freedom system via a set of equivalent single-degree-of-freedom oscillators. Superposition of modal responses is then used to compute actual system response, and the peak of that response is employed in earthquake resistant design, to construct envelopes of maximum relative responses (thus defining maximum drift), or of maximum inter-story forces. Mathematically this approach is complete, and the representation in terms of modal responses converges to the exact linear response. However, the simplifications imposed by the design practice, result in the use of only the lowest modes of response. The consequence is that the amplitudes of dynamic response to sudden,

high frequency excitation by a near-field pulse are seriously underestimated. For large strong motion amplitudes the above approach breaks down as representation in terms of a superposition of modal responses ceases to be valid for non-linear response.

When the motion of the structure can be described by one-dimensional shear beam (i.e. the contribution of rotational waves can be neglected), we have shown how equating the power of a pulse entering the structure with the ability of structure to absorb this power, PDM can lead to simple and direct estimation of required structural capacity ($a_y u_y$), via equation (20). By the example of VN7SH we showed how a push-over analysis can be used to compute this capacity $a_y u_y$.

Power (amplitude and duration) of the strong near-field pulses will determine whether the wave entering the structure will continue to propagate through the structure as a linear wave, or will begin to create non-linear zones (at first near top, and/or near base of the structure; Gicev, 2005). For high frequency pulses the non-linear zone, with permanent strains, can be created before the wave motion reaches the top of the structure, that is before the interference of waves has even started to occur leading to formation of mode shapes. Overall duration of strong motion [Trifunac and Novikova, 1994] will determine the number of times the structure may be able to complete full cycles of response, and the associated number of "minor" excursions into the non-linear response range, when the response is weakly non-linear [Gupta and Trifunac, 1996], while the presence of powerful pulses of strong motion will determine the extent to which the one-directional quarter period responses (see Eqn. (17) and Fig. 11 – center) may lead to excessive ductility demand, leading to dynamic instability and failure, precipitated by the gravity loads [Husid, 1967]. All these possibilities can be examined and quantified deterministically by computation of the associated power capacities and power demands, for different scenarios, using the PDM, for given recorded or synthesized strong motion accelerograms, or probabilistically by using the methods developed for Uniform Hazard Analysis [Todorovska et al., 1995].

5. REFERENCES

1. Akiyama, H. (1985). Earthquake-Resistant Limit-State Design for Buildings, *Univ. of Tokyo Press*, Tokyo, Japan.
2. Arias, A. (1970). A Measure of Earthquake Intensity, in "Seismic Design of Nuclear Power Plants", R.J. Hansen (editor), The Mass. Inst. of Tech. Press.
3. Benioff, H. (1934). The Physical Evaluation of Seismic Destructiveness, *Bull. Seism. Soc. Amer*., **24**, 398-403.
4. Biot, M.A. (1932). Vibrations of Building During Earthquake, Chapter II in *Ph.D. Thesis No.* 259 entitled "Transient Oscillations in Elastic Systems", Aeronautics Department, Calif. Inst. of Tech., Pasadena, California.
5. Biot, M.A. (1933). Theory of Elastic Systems Vibrating Under Transient Impulse with an Application to Earthquake – Proof Buildings, *Proc. National Academy of Sciences*, **19**(2), 262-268.
6. Biot, M.A. (1934). Theory of Vibration of Buildings During Earthquake, *Zeitschrift für Angewandte Matematik und Mechanik*, **14**(4), 213-223.

7. Biot, M.A. (1941). A Mechanical Analyzer for the Prediction of Earthquake Stresses, *Bull. Seism. Soc. Amer*., **31**(2), 151-171.

8. Biot, M.A. (1942). Analytical and Experimental Methods in Engineering Seismology, *ASCE, Transactions*, **108**, 365-408.

9. Fajfar, P. and Krawinkler, H. (editors) (1992). Nonlinear Seismic Analysis and Design of Reinforced Concrete Buildings, *Elsevier Applied Science*, London, New York.

10. Gicev, V. (2005). Investigation of soil-flexible foundation-structure interaction for incident plane SH waves, *Ph.D. Dissertation*, Dept. of Civil Engineering, Univ. Southern California, Los Angeles, California.

11. Gupta, I.D. and Trifunac, M.D. (1996)*. Investigation of Nonstationarity in Stochastic Seismic Response of Structures, *Dept. of Civil Eng. Report CE 96-01*, Univ. of Southern California, Los Angeles, California

12. Gutenberg, B. and Richter, C.F. (1956a) Earthquake Magnitude, Intensity, Energy, and Acceleration, *Bull. Seism. Soc. Amer*., **46**(2), 105-145.

13. Gutenberg, B. and Richter, C.F. (1956b). Magnitude and Energy of Earthquakes, *Ann. Geofisica*, **9**, 1-15.

14. Haskell, N.A. (1969). Elastic Displacements in the Near-Field of a Propagating Fault, *Bull. Seism. Soc. Amer*., **59**, 865-908.

15. Hayir, A., Todorovska, M.I. and Trifunac, M.D. (2001). Antiplane Response of a Dike with Flexible Soil-Structure Interface to Incident SH-waves, *Soil Dynam. and Earthquake Eng*., **21**(7), 603-613.

16. Husid, R. (1967). Gravity Effects on the Earthquake Response of Yielding Structures, *Ph.D. Thesis*, Calif. Inst. of Tech., Pasadena, California.

17. Iguchi, M., and Luco, J.E. (1982). Vibration of Flexible Plate on Viscoelastic Medium, *J. of Engrg. Mech*., ASCE, **108**(6), 1103-1120.

18. Islam, M.S. (1996). Analysis of the Response of an Instrumented 7-story Nonductile Concrete Frame Building Damaged During the Northridge Earthquake, *Professional Paper 96-9*, Los Angeles Tall Buildings Structural Design Council.

19. Ivanović, S.S., Trifunac, M.D., Novikava, E.I., Gladkov, A.A., & Todorovska, M.I. (1999)*. Instrumented 7-story Reinforced Concrete Building in Van Nuys, California: Ambient Vibration Surveys Following the Damage from the 1994 Northridge Earthquake. Dept. of Civil Eng., *Rep. No. CE 99-03*, Univ. of Southern California, Los Angeles, California.

20. Ivanović, S.S., Trifunac, M.D., Novikava, E.I., Gladkov, A.A., & Todorovska, M.I. (2000). Ambient Vibration Tests of a Seven-Story Reinforced Concrete Building in Van Nuys, California, Damaged by the 1994 Northridge Earthquake. *Soil Dynam. and Earthquake Engrg*., **19**(6), 391-411.

21. Joyner, W.B. (1975). A Method for Calculating Nonlinear Seismic Response in Two Dimensions, *Bull. Seism. Soc. Amer*., **65**(5), 1337-1357.

22. Joyner, W.B. and Chen, A.T.F. (1975). Calculating of Nonlinear Ground Response in Earthquakes, *Bull. Seism. Soc. Amer*., **65**(5), 1315-1336.

23. Kanai, K. (1965). Some problems of seismic vibration of structures, Proc. Third World Conf. Earthquake Eng., New Zealand, Vol. II, 260-275.

24. Lee, V.W. (1979)*. Investigation of Three-Dimensional Soil-Structure Interaction, *Report No. CE 79-11*, Dept. of Civil Eng., University of Southern California, Los Angeles, California.

25. Lee, V.W., Trifunac, M.D. and Feng, C.C. (1982). Effects of Foundation Size on Fourier Spectrum Amplitudes of Earthquake Accelerations Recorded in Buildings, Soil Dynam. and Earthquake Eng., **1**(2), 52-58.

26. Li, R.Y. and Jirsa, J.D. (1998). Nonlinear Analysis of an Instrumented Structure Damaged in the 1994 Northridge Earthquake, *Earthquake Spectra*, **14**(2), 265-283.

27. Luco, J.E., M.D. Trifunac and Wong, H.L. (1985)*. Soil Structure Interaction Effects on Forced Vibration tests, Dept. of Civil Eng. *Report No. 86-05*, Univ. of Southern California, Los Angeles, California.

28. Moslem, K. and Trifunac, M.D. (1987). Spectral Amplitudes of Strong Earthquake Accelerations Recorded in Buildings, *Soil Dynam. and Earthquake Eng*., **6**(2), 100-107.

29. Richter, C.F. (1936). An Instrumental Earthquake Magnitude Scale, *Bull. Seism. Soc. Amer*., **25**, 1-32.

30. Richter, C.F. (1958). Elementary Seismology, *Freeman and Co*., S. Francisco.

31. Safak, E. (1998). New Approach to Analyzing Soil-Building Systems, *Soil Dynam. and Earthquake Eng*,, **17**, 509-517.

32. Todorovska, M.I., and Lee, V.W. (1989). Seismic Waves in Buildings with Shear Walls or Central Core, *J. Engrg. Mech*., ASCE, **115**(12), 2669-2686.

33. Todorovska, M.I., and Trifunac, M.D. (1989). Antiplane Earthquake Waves in Long Structures, *J. of Engrg. Mech*., ASCE, **115**(12), 2687-2708.

34. Todorovska, M.I., and Trifunac, M.D. (1990a). A Note on the Propagation of Earthquake Waves in Buildings with Soft First Floor, *J. of Engrg. Mech*., ASCE, **116**(4), 892-900.

35. Todorovska, M.I., and Trifunac, M.D. (1990b). A Note on Excitation of Long Structures by Ground Waves, *J. of Engrg Mech*., ASCE, **116**(4), 952-964.

36. Todorovska, M.I. and Trifunac, M.D. (1990c)*. Analytical Model for In-plane Building-Foundation-Soil Interaction: Incident P-, SV- and Rayleight Waves, Dept. of Civil Engrg, *Report No. 90-01*, Univ. of Southern California, Los Angeles, California.

37. Todorovska, M.I. and Trifunac, M.D. (1991)*. Radiation Damping During Two-Dimensional Building-Soil Interaction, Dept. of Civil Eng., *Rep. No. 91-01*, Univ. of Southern California, Los Angeles, California.

38. Todorovska, M.I. and Trifunac, M.D. (1992). The System Damping, the System Frequency and the System Response peak Amplitudes during in-plane Building-Soil Interaction, *Earthquake Eng. and Struct. Dynam.*, **21**(2), 127-144.

39. Todorovska, M.I. and Trifunac, M.D. (1993)*. The Effects of Wave Passage on the Response of Base-Isolated Buildings on Rigid Embedded Foundations, Dept of Civil Eng., *Report No. CE 93-10*, Univ. of Southern California, Los Angeles, California.

40. Todorovska, M.I. and Trifunac, M.D. (1997a). Distribution of Pseudo Spectral Velocity During the Northridge, California, Earthquake of 17 January, 1994, *Soil Dynam. and Earthquake Eng*., **16**(3), 173-192.

41. Todorovska, M.I. and Trifunac, M.D. (1997b). Amplitudes, Polarity and Times of Peaks of Strong Ground Motion During the 1994 Northridge, California Earthquake, *Soil Dynam. and Earthquake Eng*., **16**(4), 235-258.

42. Todorovska, M.I., Trifunac, M.D. , and Lee, V.W. (1988)*. Investigation of Earthquake Response of Long Buildings, Dept of Civil Engrg, *Report No. CE 88-02*, Univ. of Southern California, Los Angeles, California.

43. Todorovska, M.I., Gupta, I.D., Gupta, V.K., Lee, V.W., and Trifunac, M.D. (1995)*. Selected Topics in Probabilistic Seismic Hazard Analysis, *Dept. of Civil Eng. Report CE 95-08*, Univ. of Southern California, Los Angeles, California.

44. Todorovska, M.I. Ivanovic, S.S. and Trifunac, M.D. (2001a). Wave Propagation in a Seven-Story Reinforced Concrete Building, Part I: Theoretical Models, *Soil Dynam. and Earthquake Eng*., **21**(3), 211-223.

45. Todorovska, M.I. Ivanovic, S.S. and Trifunac, M.D. (2001b). Wave Propagation in a Seven-Story Reinforced Concrete Building, Part II: Observed Wave Numbers, *Soil Dynam. and Earthquake Eng*., **21**(3), 211-223.

46. Todorovska, M.I., Hayir, A. and Trifunac, M.D. (2001c). Antiplane Response of a Dike on Flexible Embedded Foundation to Incident SH-Waves, *Soil Dynam. and Earthquake Eng*., **21**(7), 593-601.

47. Trifunac, M.D. (1972a). Stress Estimates for San Fernando, California Earthquake of February 9, 1971: Main Event and Thirteen Aftershocks, *Bull Seism. Soc. Amer.*, **62**, 721-750.

48. Trifunac, M.D. (1972b). Tectonic Stress and Source Mechanism of the Imperial Valley, California Earthquake of 1940, *Bull. Seism. Soc. Amer*., **62**, 1283-1302.

49. Trifunac, M.D. (1972c) Interaction of a Shear Wall with the Soil for Incident Plane SH Waves, *Bull. Seism. Soc. Amer*., **62**, 63-83.

50. Trifunac, M.D. (1974). A Three-Dimensional Dislocation Model for the San Fernando, California, Earthquake of February 9, 1971, *Bull. Seism. Soc. Amer*., **64**, 149-172.

51. Trifunac, M.D. (1989). Dependence of Fourier Spectrum Amplitudes of Recorded Strong Earthquake Accelerations on Magnitude, Local Soil Conditions and on Depth of Sediments, *Earthquake Eng. and Struct. Dynam*., **18**(7), 999-1016.

52. Trifunac, M.D. (1991). M_L^{SM} , *Soil Dynam. and Earthquake Eng*., **10**(1), 17-25.

53. Trifunac, M.D. (1993). Long Period Fourier Amplitude Spectra of Strong Motion Acceleration, *Soil Dynam. and Earthquake Eng*., **12**(6), 363-382.

54. Trifunac, M.D. (1994). Q and High Frequency Strong Motion Spectra, *Soil Dynam. and Earthquake Eng*., **13**(3), 149-161.

55. Trifunac, M.D. (1998). Stresses and Intermediate Frequencies of Strong Motion Acceleration, *Geofizika*, **14**, 1-27.

56. Trifunac, M.D. (2003)*. 70-th Anniversary of Biot Spectrum, 23-rd Annual ISET Lecture, *Indian Society of Earthquake Technology*, Vol. 40, No. 1, 19-50.

57. Trifunac, M.D. (2005). Scientific citations of M. A. Biot, Proc. Biot centennial conference, Norman, Oklahoma, in *Poromechanics III,* Edited by Abousleiman, Y.N., Cheng, A.H., and Ulm, F.J., 11-17, (2005).

58. Trifunac, M.D. and Brady, A.G. (1975a). A Study of the Duration of Strong Earthquake Ground Motion, *Bull. Seism. Soc. Amer*., **65**, 581-626.

59. Trifunac, M.D. and Brady, A.G. (1975b). On the Correlation of Seismic Intensity Scales with the Peaks of Recorded Strong Ground Motion, *Bull. Seism. Soc. Amer*., **65**, 139-162.

60. Trifunac, M.D. and Novikova, E.I., (1994). State of the Art Review on Strong Motion Duration, *10th European Conf. on Earthquake Eng*., Vol. I, 131-140.

61. Trifunac, M.D. and Todorovska, M.I. (1996). Nonlinear Soil Response – 1994 Northridge California, Earthquake, *J. Geotechnical Eng.,* ASCE, **122**(9), 725-735

62. Trifunac, M.D. and Todorovska, M.I. (1997). Northridge, California, Earthquake of January 17, 1994: Density of Red-Tagged Buildings Versus Peak horizontal Velocity and Site Intensity of Strong Motion, *Soil Dynam. and Earthquake Eng*., **16**(3), 209-222.

63. Trifunac, M.D. and Todorovska, M.I. (1998). Nonlinear Soil Response as a Natural Passive Isolation Mechanism – The 1994 Northridge, California Earthquake, *Soil Dynam. and Earthquake Eng*., **17**(1), 41-51.

64. Trifunac, M.D. and Todorovska, M.I. (1999). Reduction of Structural Damage by Nonlinear soil Response, *J. Structural Eng.,* ASCE, **125**(1), 89-97.

65. Trifunac, M.D. and Todorovska, M.I. (2001). Recording and Interpreting Earthquake Response of Full-Scale Structures, Proc. NATO Workshop on Strong Motion Instrumentation for Civil Engineering Structures, June 2-5, 1999, Instanbul, Turkey, M. Erdik et al. (eds.), *Kluwer Academic Publishers*, 131-155.

66. Trifunac, M.D., Todorovska, M.I. and Lee, V.W. (1998). The Rinaldi Strong Motion Accelerogram of the Northridge, California, Earthquake of 17 January, 1994, *Earthquake Spectra*, **14**(1), 225-239.

67. Trifunac, M.D., Ivanovic, S.S., Todorovska, M.I., Novikova, E.I. and Gladkov, A.A. (1999a). Experimental Evidence for Flexibility of a Building Foundation Supported by Concrete Friction Piles, *Soil Dynam. and Earthquake Eng*., **18**(3), 169-187.

68. Trifunac, M.D., Ivanovic, S.S. and Todorovska, M.I. (1999b)*. Seven Story Reinforced Concrete Building in Van Nuys, California: Strong Motion Data Recorded Between 7 February 1971 and 9 December 1994, and Description of Damage Following Northridge, 17 January 1994 Earthquake, Dept. of Civil Eng., *Rep. No. 99-02*, Univ. of Southern California, Los Angeles, California.

69. Trifunac, M.D., Ivanovic, S.S. and Todorovska, M.I. (2001a). Apparent Periods of a Building, Part I: Fourier Analysis, *J. of Structural Eng*., ASCE, **127**(5), 517-526.

70. Trifunac, M.D., Ivanovic, S.S. and Todorovska, M.I. (2001b). Apparent Periods of a Building, Part II: Time-Frequency Analysis, *J. of Structural Eng*., ASCE, **127**(5), 527-537.

71. Trifunac, M.D., Todorovska, M.I. and Hao, T.Y. (2001c). Full-Scale Experimental Studies of Soil-Structure Interaction – A Review, *Proc. 2nd U.S.-Japan Workshop on Soil-Structure Interaction*, March 6-8, Tsukuba City, Japan.

72. Trifunac, M.D., Ivanovic, S.S. and Todorovska, M.I. (2001d). Wave Propagation in a Seven-story Reinforced Concrete Building, III: Damage Detection Via Changes in Wave Numbers, *Soil Dynam. and Earthquake Eng.*, **23**(1), 65-75.

73. Trifunac, M.D., Hao, T.Y. and Todorovska, M.I. (2001e)*. On Energy Flow in Earthquake Response, Dept. of Civil Eng., *Report No. CE 01-03*, Univ. of Southern California, Los Angeles, California.

74. Uang, C.M., & Bertero, V.V. (1988). Use of Energy as a Design Criterion in Earthquake-Resistant Design. *Report No. UCB/EERC-88/18*, Earthquake Engineering Research Center, University of California, Berkeley, California.

---

*Can be downloaded from: http://www.usc.edu/dept/civil_eng/Earthquake_eng/